J Physiol (2003), **551.1**, *pp.* 139–153

DOI: 10.1113/jphysiol.2003.044784
www.jphysiol.org

Journal of Physiology

Pyramidal cell communication within local networks in layer 2/3 of rat neocortex

Carl Holmgren, Tibor Harkany*, Björn Svennenfors and Yuri Zilberter

*Karolinska Institute, Department of Neuroscience, Retzius väg 8, B2-2, S-17177 and *Laboratory for Molecular Neurobiology, Department of Medical Biochemistry and Biophysics, Scheeles väg 1, A1, Karolinska Institute, S-17177 Stockholm, Sweden*

The extent to which neocortical pyramidal cells function as a local network is determined by the strength and probability of their connections. By mapping connections between pyramidal cells we show here that in a local network of about 600 pyramidal cells located within a cylindrical volume of 200 μm × 200 μm of neocortical layer 2/3, an individual pyramidal cell receives synaptic inputs from about 30 other pyramidal neurons, with the majority of EPSP amplitudes in the 0.2–1.0 mV range. The probability of connection decreased from 0.09 to 0.01 with intercell distance (over the range 25–200 μm). Within the same volume, local interneuron (fast-spiking non-accomodating interneuron, FS)–pyramidal cell connections were about 10 times more numerous, with the majority of connections being reciprocal. The probability of excitatory and inhibitory connections between pyramidal cells and FS interneurons decreased only slightly with distance, being in the range 0.5–0.75. Pyramidal cells in the local network received strong synaptic input during stimulation of afferent fibres in layers 1 and 6. Minimal-like stimulation of layer 1 or layer 6 inputs simultaneously induced postsynaptic potentials in connected pyramidal cells as well as in pyramidal–FS cell pairs. These inputs readily induced firing of pyramidal cells, although synaptically connected cells displayed different firing patterns. Unitary EPSPs in pyramidal–pyramidal cell pairs did not detectably alter cell firing. FS interneurons fire simultaneously with pyramidal cells. In pyramidal–FS cell pairs, both unitary EPSPs and IPSPs efficiently modulated cell firing patterns. We suggest that computation in the local network may proceed not only by direct pyramidal–pyramidal cell communication but also via local interneurons. With such a high degree of connectivity with surrounding pyramidal cells, local interneurons are ideally poised to both coordinate and expand the local pyramidal cell network via pyramidal–interneuron–pyramidal communication.

(Resubmitted 8 April 2003; accepted after revision 22 May 2003; first published online 17 June 2003)
Corresponding author Y. Zilberter: Karolinska Institute, Department of Neuroscience, Retzius väg 8, B2-2, S-17177 Stockholm, Sweden. Email: yuri.zilberter@neuro.ki.se

Communication relies on the use of a common system of signs or behaviours. Within the neocortex this occurs through the exchange of information locally and inter-areally using neuronal code in the form of spike trains. Pyramidal cell communication in layer 2/3 represents the response of these cells to afferent and local network signals. The role of local pyramidal cells in the shaping of pyramidal cell firing is determined by their functional connectivity. This process presumably underlies information processing within the neocortex, the understanding of which is one of the principal goals of modern neuroscience.

Dual recordings from pyramidal cells in the same layer of rat neocortex (Mason *et al.* 1991; Markram *et al.* 1997; Thomson & Deuchars, 1997; Gibson *et al.* 1999; Reyes & Sakmann, 1999; Thomson *et al.* 2002) or different cortical layers (Thomson & Deuchars, 1997; Reyes & Sakmann, 1999; Thomson *et al.* 2002) indicated that pyramidal cells have low local interconnectivity. Intralaminar pyramidal connection ratios in layer 2/3 of 1:10 (Mason *et al.* 1991) or 1:4 (Thomson *et al.* 2002), and in layer 3 of 1:21 (Thomson & Deuchars, 1997) have been reported. Interlaminar connection ratios of 1:86 (Thomson & Deuchars, 1997) or 1:29 (Thomson *et al.* 2002) (layer 5 to 3) have been found. Additionally, the efficacy of synaptic connections between pyramidal cells in layer 2/3 is low with mean amplitudes of 0.55 mV (Mason *et al.* 1991), 0.3–0.5 mV (Reyes & Sakmann, 1999), 1 mV (Thomson & Deuchars, 1997) and 1.7 mV (Thomson *et al.* 2002) recorded. The difference in the results obtained may be related to the different ages of animals used and/or different techniques employed.

Knowing the overall pyramidal–pyramidal cell connectivity ratio within a region is, however, insufficient for the evaluation of the common contribution of pyramidal cells within a local network to the excitability of each network member. For this purpose, an essential additional parameter is required. This is the dependence of connection probability on the distance between cells. Estimation of the number of connected pyramidal cells within a fixed cortical volume is

not possible until this function is known. Evidently, a large number of pyramidal cells acting in unison, even with low interneuronal synaptic efficacy, may provide a significant excitatory effect. In spite of the attempts to estimate the dependence of connection probability on the distance between cells, by morphological reconstruction of neurons (see, for example, Hellwig, 2000), direct measurements of this important function have not been reported so far.

In order to provide a quantitative analysis of pyramidal cell functional connectivity in layer 2/3 of the neocortex we therefore mapped pyramidal–pyramidal, and pyramidal–fast-spiking non-accomodating interneuron (FSN) (Zilberter, 2000) connections, noting both the radial and tangential location of each cell sampled. FSN interneurons represent a sub-population of fast-spiking (FS) interneurons extensively described elsewhere (Connors & Gutnik, 1990; Kawaguchi, 1995; Cauli *et al.* 1997; Gupta *et al.* 2000; Wang *et al.* 2002), and the term FS will therefore be used in the text.

The major questions we address in this study are: (1) what is the contribution of pyramidal cells constituting the local network to excitability of a single pyramidal cell? (2) how intense is the connectivity of an inhibitory interneuron (FS) with pyramidal cells in the local network? (3) how effective is unitary excitatory and inhibitory synaptic signalling in modulating neuronal firing in the local network?

Individual neurons *in vivo* receive intense synaptic input and generate apparently random spike trains (for review see Steriade, 2001). Synchronous afferent inputs can induce neuronal firing with high variability (Stevens & Zador, 1998). The intense synaptic input strongly affects the input resistance of neurons (Borg-Graham *et al.* 1998; Pare *et al.* 1998; Destexhe & Pare, 1999), changing their integration properties (Bernander *et al.* 1991; Destexhe & Pare, 1999; London & Segev, 2001). Using the dynamic clamp technique (Sharp *et al.* 1993) and a 'point conductance' model, Destexhe *et al.* (2001) recreated *in vivo*-like activity in slices. However, the *in vivo* pattern of dendritic integration is difficult to reproduce using somatic current injection due to the non-compact electrotonic structure of the pyramidal neurons. Thus, to address the effects of strong synaptic activity and synchronous afferent inputs, we mimicked these *in vivo* conditions by simultaneously applying random stimulation independently to afferent fibres in layer 1 (L1) and layer 6 (L6), which provide strong synaptic inputs to neurons in layer 2/3 (Cauller & Connors, 1994). Of course, in the living animal, the order of recruitment of presynaptic elements might be quite different to extracellulary evoked random input. However, afferent random stimulation enabled the initiation of cell firing under conditions of dendritic integration mimicking those *in vivo*. This allowed us to test in slices how synaptic signalling, including unitary signalling, can modulate pyramidal cell firing.

METHODS

Electrophysiological measurements

Cortical parasagittal or coronal slices (300 μm) were prepared from 14- to 16-day-old Sprague-Dawley rats (Markram *et al.* 1997). Animals were killed by rapid decapitation, in accordance with the ethical guidelines of the Karolinska Institute. Neurons in layer 2/3 of visual and somatosensory neocortical areas were selected on the basis of morphological features using infrared-differential interference contrast video microscopy and subsequent characterization of neuron firing properties. The extracellular solution contained (mM): 125 NaCl, 2.5 KCl, 2 $CaCl_2$, 1 $MgCl_2$, 25 $NaHCO_3$, 1.25 NaH_2PO_4 and 25 glucose. The pipette solution contained (mM): 125 potassium gluconate, 20 KCl, 4 ATP-Mg, 10 sodium phosphocreatine, 0.3 GTP and 10 Hepes, pH 7.3. Experiments were performed at 32–34 °C. All measurements affected by inhibitory components were performed with a low Cl^- (1 or 4 mM) intracellular solution, with the potassium gluconate concentration adjusted accordingly.

Recordings were made using Axopatch 200B and Axoclamp 2B amplifiers (Axon Instruments, Foster City, CA, USA), and sampled at intervals between 50 and 100 μs, digitized by an ITC-18 interface (Instrutech, Port Washington, NY, USA) and stored on the hard disk of a Macintosh computer for off-line analysis (IGOR-Pro, Wavemetrics Inc., Lake Oswego, OR, USA). Patch pipettes were made from borosilicate glass and had a resistance of 3–5 MΩ. Series resistance was not compensated.

During mapping of cell connectivity, one pipette was kept immobile (in the case of FS–pyramidal recordings this was the FS interneuron pipette) while the second pipette was used to sample pyramidal cells (in the range of 1 to 14).

When calculating pyramidal–pyramidal cell connecting probability, cell pairs with no connection in either direction were counted as two connection failures; pairs in which a uni-directional connection was found were counted as one connection and one connection failure; and pairs with reciprocal connections were counted as two connections.

Bipolar electrodes (25 μm platinum–iridium wire) $>$ 1 mm lateral, in the case of layer 1 stimulation, and $<$ 400 μm lateral, in the case of layer 6, to the recorded cell (see Fig. 4*A*) were used for extracellular stimulation. Two sets of 40 random stimulus trains (500 ms each) with a minimal interspike interval of 5 ms were created using a Gaussian random number pulse generator in custom-made software (IGOR-Pro). Stimulus trains (0.5–4 mA) were applied by two isolating stimulators (A360; WPI, Sarasota, FL, USA) independently and simultaneously to layers 1 and 6 every 10 s. To eliminate possible effects of time-dependent changes, all experiments were conducted with a cyclical control–test–control pattern for the duration of the experiment. In all experiments where results during random L1 and L6 stimulation were compared, the same patterns of random stimulation were used in control and testing.

The pyramidal cell input resistance calculated from current–voltage relationships, measured by a series of 500 ms small current injections at the resting potential (RP) level, was 197 ± 38.5 MΩ (n = 14). Similar measurements in FS interneurons showed an input resistance of 145 ± 24.1 MΩ (n = 10).

Unitary EPSPs or IPSPs were measured in averaged records from at least 50 sweeps. Extracellularly evoked EPSPs were measured in averaged records from at least 30 sweeps.

The paired-pulse ratio was calculated as PSP2/PSP1, where PSP1 and PSP2 were average postsynaptic potential amplitudes in response to the first and second action potentials in a presynaptic cell (100 ms interpulse interval). When necessary, the decay phase of the first PSP was extrapolated to provide a baseline for measuring the second PSP amplitude.

For correlation analysis, action potentials (APs) in each original voltage trace were approximated by 2 ms rectangular pulses with an amplitude of 1, and the baseline level with an amplitude of 0. In a series of experiments, cross-correlation was used for testing the influence of unitary synaptic signalling on the firing of postsynaptic cells. Cell firing was evoked by extracellular stimulation of L1 and L6. Postsynaptic cell firing was analysed with or without somatic hyperpolarization of the presynaptic cell preventing its firing. In both cases, firing of the postsynaptic cell was analysed for correlation with that of the presynaptic cell recorded in the absence of hyperpolarization. Then two cross-correlograms were compared.

Average data are given as means ± S.D. unless otherwise stated. Statistical significance was tested using Student's paired *t* test.

Reconstruction of identified neurons by confocal laser-scanning microscopy

Cells were intracellularly labelled with biocytin (0.5 mg ml^{-1}) through the patch pipette for 10–20 min. Special care was taken to select cells at a tissue depth identical to that of cells used for electrophysiological recordings.

Slices were immersion-fixed in 4 % paraformaldehyde and 0.1 % glutaraldehyde in phosphate buffer (PB, 0.1 M, pH 7.4) overnight. After repeated washes in PB, slices were incubated in a solution containing 0.25 μg ml^{-1} carbocyanine 3 (Cy3)-conjugated streptavidin (affinity-purified; Jackson Immunoresearch, West Grove, PA, USA), 0.5 % Triton X-100 in PB for 16 h at 4 °C. After subsequent rinses in PB, slices were dipped in distilled water, mounted on fluorescence-free glass slides and dried at room temperature. Subsequently, slices were coverslipped with Entellan (in toluene; Merck, Darmstadt, Germany).

To identify major morphological characteristics of both pyramidal cells and interneurons, identified nerve cells were inspected using a Zeiss 510 confocal laser-scanning microscope (Zeiss, Jena, Germany) equipped with a helium–neon laser (543 nm) and an appropriate band-pass filter (560–610 nm) for selective detection of Cy3 signal. To reach maximum resolution in a 200 μm radius around the identified neurons in reconstruction analyses, × 20 primary magnification was used (460.6 μm × 460.6 μm field of view), and the entire slice thickness containing the fluorescence signal, including both surfaces, was sampled along the *z*-axis (41.06 ± 3.97 μm). Because of extensive drying and subsequent coverslipping of our specimen, approximately 3.5-fold shrinkage of tissue was observed. When correcting for shrinkage in image analysis, the sampled tissue depth amounted to ~140–150 μm. Pinhole and stepwise *z*-stack settings were both set to 1.3 μm, which allowed an appropriate signal to noise ratio to visualize fine boutons and their possible cuts, without loss of signal in any of the sampling fields.

To determine whether arbors of pyramidal cells ($n = 7$) sustained extensive damage during slice preparation, images of individual confocal planes of each cell were merged. Cuts of axons and dendrites appeared as bright red dots on the tissue surface. Axons were distinguished from dendrites by their smooth appearance and lack of dendritic spines. Subsequently, projection images were exported in high-resolution tagged image format (TIFF) and processed in Paint Shop Pro (version 7.0.1, Jasc Software Inc., Eden Prairie, MN, USA) to yield reconstruction of pyramidal cells and inhibitory neurons (Fig. 1).

RESULTS

Minimizing axonal cutting

Axonal cutting during brain slicing may severely affect cell connectivity tested in slices. To minimize this effect, we made use of the fact that pyramidal cells in sequential parasagittal slices show a change in their orientation with respect to the cut slice surface. In each experiment, a slice

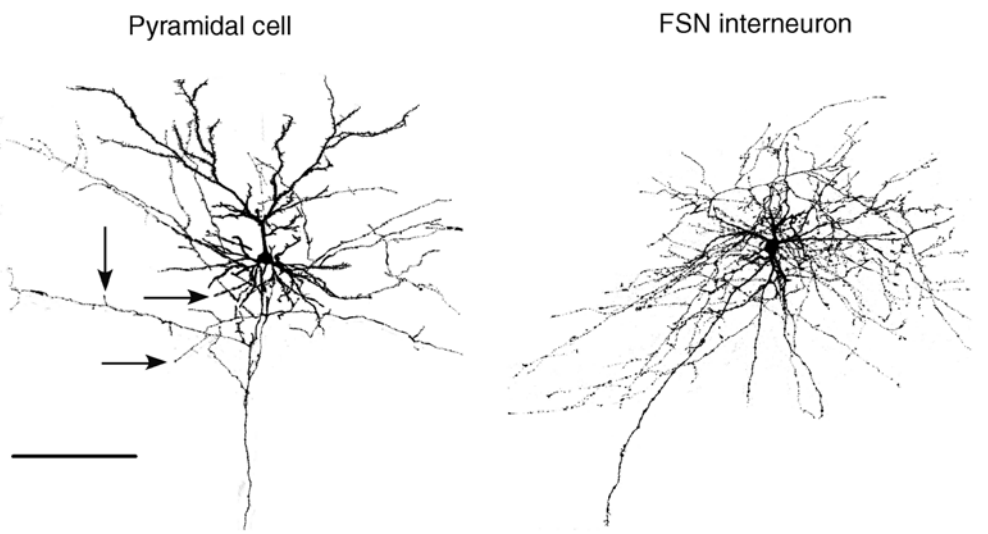

Figure 1. A representative pyramidal cell and interneuron after reconstruction using confocal laser-scanning microscopy

Images were taken over a 460.6 μm × 460.6 μm surface area. Arrows point to cuts in the pyramidal cell axon. Scale bar = 200 μm.

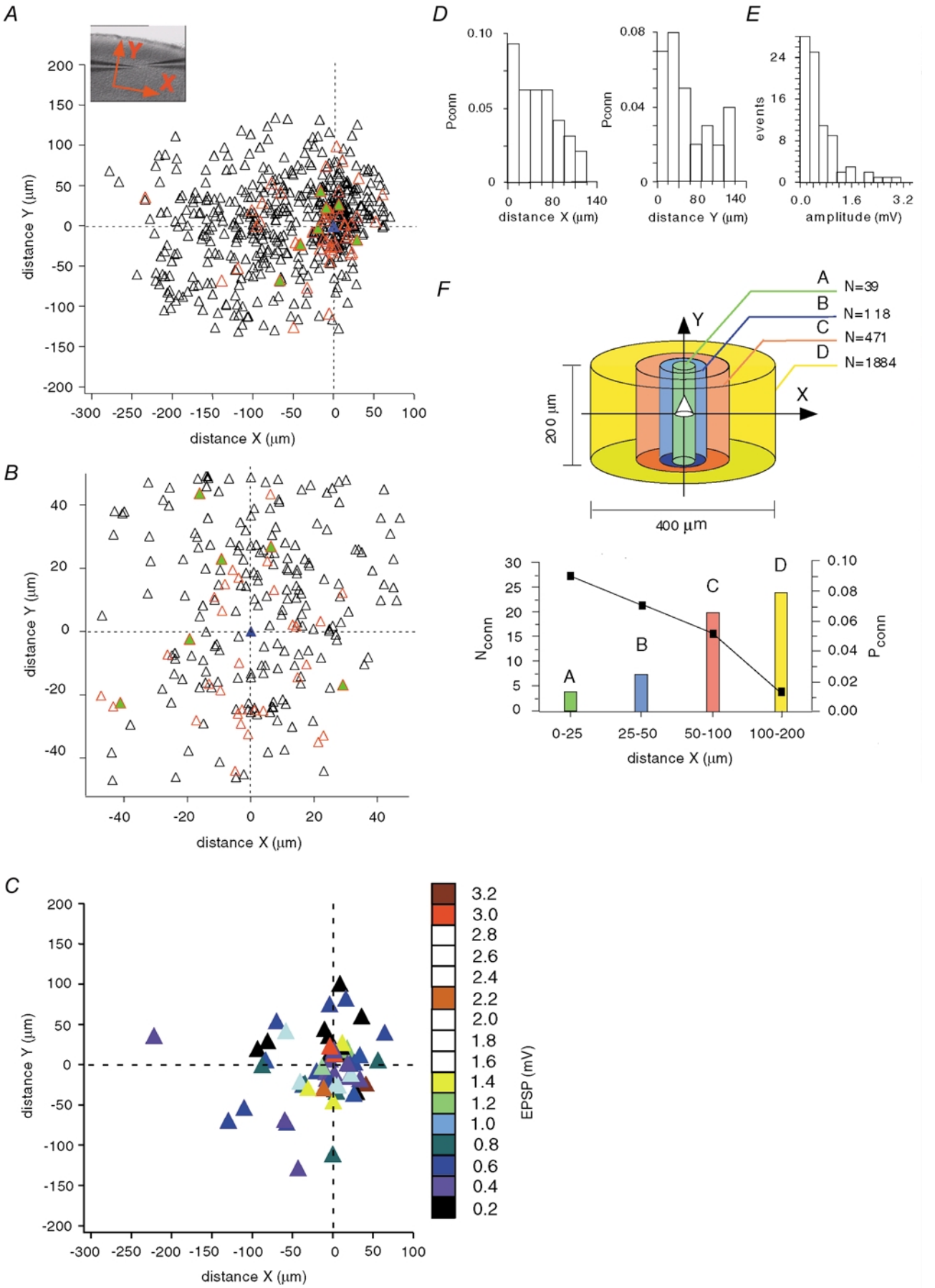

Figure 2. For legend see facing page.

with pyramidal cell apical dendrites parallel to the cut slice surface was located. The subsequent one to three slices, which had pyramidal cell apical dendrites ascending towards the cut surface, and axons descending into the slice, were selected. Cell somata were located at depths > 40 μm. Camera lucida reconstruction of 18 pyramidal cells filled with biocytin confirmed that in all cases the major axonal branches were intact, with minor damage to vertically oriented collaterals in a few instances.

To unequivocally identify whether cuts on axonal branches of excitatory neurons were a critical modifying factor in our experiments, pyramidal cells were visualized using a neurobiotin–Cy3-conjugated streptavidin system and reconstructed using confocal laser-scanning microscopy. Special attention was given to a sample field of 200 μm radius around each cell, as subsequent paired electrophysiological recordings were undertaken within this surface area. Projection of adjacent images along the dorsoventral axis in the slices revealed cuts on only tertiary and quaternary axon collaterals (number of cuts: 3.43 ± 0.58 (mean ± S.E.M.) per neuron, $n = 7$; Fig. 1), whereas the main axon stem remained intact. It is noteworthy that multiple, intact, descending axon branches were traced to layers 5/6. FS interneurons were reconstructed in a manner identical to that of pyramidal cells, although without analysis of the number of cuts on their axons (Fig. 1). Cell somata were situated at an average depth of 45–50 μm.

Pyramidal–pyramidal cell connectivity

A map of pyramidal cell connections representing 542 cell pairs tested in layer 2/3 of the neocortex is shown in Fig. 2*A*. The inset demonstrates the orientation of the *X*- and *Y*-axes in a slice. We limited our study to the cortical volume of a 400 μm × 200 μm cylinder (see Fig. 2*F*). The blue triangle with (0, 0) coordinates in Fig. 2*A* corresponds to a cell (central cell) patched with the immobile pipette or, in the case of a synaptic connection, to the postsynaptic cell. Synaptic connections were found in 61 cell pairs (red triangles), with 7 pairs connected reciprocally (green filled triangles). All other cells, depicted as black triangles, were not connected. The highest density of connected cells was found in close proximity (±25 μm in the *X*-direction, ±50 μm in the *Y*-direction, Fig. 2*B*) to the central cell. Figure 2*D* shows the distribution of connection probability in the *X*- and *Y*-directions. The distribution of EPSP amplitudes (Fig. 2*E*) reveals that the efficacy of these connections was relatively weak, with the majority of EPSP amplitudes in the 0.2–1.0 mV range. In a few cases, however, much stronger synaptic connections were found (2.1–3.3 mV, $n = 5$). The average EPSP amplitude was 0.65 ± 0.64 mV. Figure 2*C* shows the corresponding map of EPSP amplitudes. The strongest connections were observed between closely positioned pyramidal cells, although the small number of distant connections is insufficient to draw any conclusions.

To test whether pyramidal cell connectivity is different in antero-posterior and medio-lateral planes we performed an additional series of experiments using coronal slices. In 110 cell pairs located within 100 μm of each other, we found eight connected cell pairs including two connected reciprocally. This suggests the lack of a significant difference in pyramidal cell connectivity in perpendicular planes. Thus, using parasagittal slices we did not severely affect the network by cutting connections between pyramidal cells.

Some mapping experiments (about 12 %) were performed using 400 μm slices and did not show a significant difference in cell connectivity.

To estimate the number of synaptic inputs a pyramidal cell can receive from other pyramidal cells within the local network, it is necessary to know the pyramidal cell density. Cell density in the rat visual cortex remains stable after postnatal day 12 (Nunez *et al.* 2001). We used an overestimate of 100 000 pyramidal cells mm^{-3} in the following calculations (range reported previously 32 000–87 000 mm^{-3} (Peters & Kara, 1985; Peters *et al.* 1985; Gabbott & Stewart, 1987; Miki *et al.* 1995, 1997). This allowed us to compensate, at least partially, for the possible loss of synaptic connections due to axonal cutting. Since connection probability was strongly dependent on the *X*-distance, decreasing from 0.09 within ±25 μm from the central cell to 0.01 at

Figure 2. Mapping of pyramidal cell connections in layer 2/3 of neocortex

A, the inset demonstrates the orientation of *X*- (tangential) and *Y*- (radial) axes in a slice. The blue triangle with (0, 0) coordinates corresponds to a pyramidal cell patched with the immobile pipette or, in the case of a synaptic connection, to the postsynaptic cell. From 542 cell pairs, synaptic connections were found in 61 cell pairs (red triangles), with 7 pairs connected reciprocally (green filled triangles). All other cells, depicted as black triangles, were not connected. *B*, the area of highest cell density, from Fig. 1*A*, on an expanded scale. *C*, mapping of EPSP amplitudes of connected pyramidal cells. Numbers on the scale bar on the right show the maximal EPSP amplitude represented by each coloured square. *D*, connection probability (P_{conn}), with distance, of pyramidal cells in the tangential (*X*) and radial (*Y*) directions. *E*, distribution of EPSP amplitudes in pyramidal–pyramidal cell pairs. *F*, upper panel, numbers in the diagram (*N*) show the total pyramidal cell number that would be in each volume (values calculated taking a pyramidal cell density of 100 000 pyramidal cells mm^{-3}). Lower panel, connection probability (P_{conn}), from the mapping of pyramidal connectivity (*A*), depending on the distance between cells (black rectangles) and the calculated number of pyramidal cells synaptically connected (N_{conn}) to a single postsynaptic pyramidal cell (bars) in volumes shown in the upper panel.

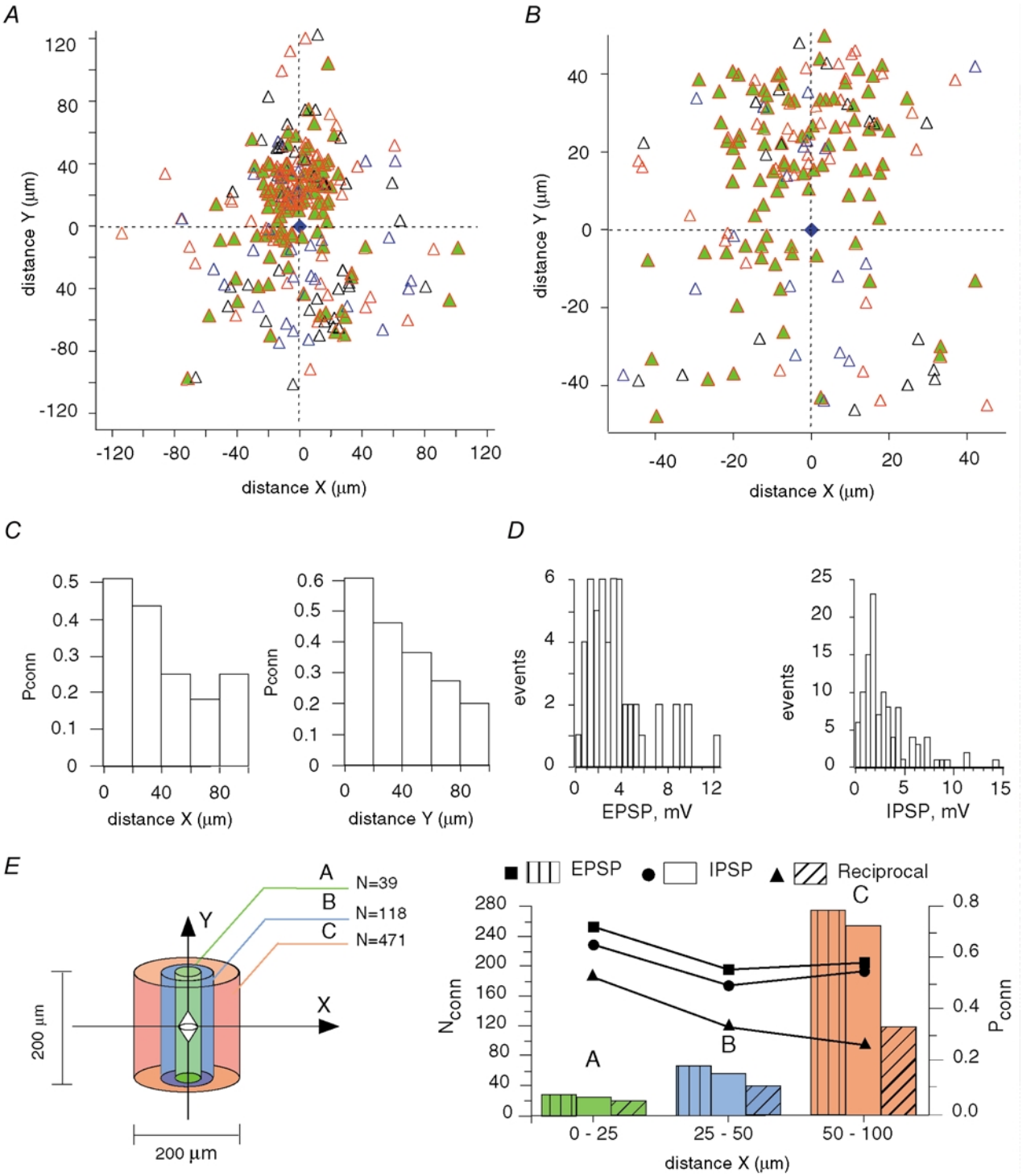

Figure 3. Mapping of pyramidal–interneuron (FS) connections in layer 2/3 of neocortex

A, the interneuron (blue trapezium) is set in the centre (0, 0) with pyramidal cells depicted as triangles. In most cases, pyramidal cells innervated FS neurons (red triangles). Moreover, the majority of connections were reciprocal (green filled triangles). Blue triangles correspond to the unidirectional inhibitory connections. *B*, central part of the map with dimensions similar to those in Fig. 2*B* for pyramidal cells. Contrary to pyramidal–pyramidal cell connectivity, the majority of pyramidal cells are interconnected with the interneuron. *C*, connection probability (P_{conn}), with distance, of reciprocal pyramidal–FS connections in the tangential (*X*) and radial (*Y*) directions. *D*, distributions of EPSP and IPSP amplitudes measured at resting potential. *E*, left, numbers (*N*) in the diagram show the total pyramidal cell number that would be in each volume, calculated by taking a pyramidal cell density of 100 000 pyramidal cells mm^{-3} (FS cell central). Right, probabilities (P_{conn}), from the mapping of pyramidal–FS connectivity (*A*), of excitatory (rectangles), inhibitory (circles) and reciprocal (triangles) connections. Bars indicate the calculated number of corresponding connections (N_{conn}) formed by the interneuron with pyramidal cells in the volumes shown on the left.

Table 1. Properties of synaptic connections in pyramidal–pyramidal and pyramidal–FS cell pairs

Connection	EPSP/IPSP at RP (mV)	10–90% rise time (ms)	Width at half-amplitude (ms)	Paired-pulse ratio**
Pyramidal–pyramidal	0.65 ± 0.64 (n = 83)	5.28 ± 1.88 (n = 15)	36.46 ± 16.55 (n = 15)	0.92 ± 0.42 (n = 70)
Pyramidal–FS	3.48 ± 2.52 (n = 79)	2.32 ± 1 (n = 17)	16.25 ± 5.78 (n = 17)	0.7 ± 0.14 (n = 20)
FS–pyramidal	2.96 ± 2.52* (n = 109)	6.5 ± 3.67 (n = 32)	55.9 ± 22.6 (n = 32)	0.7 ± 0.15 (n = 22)

* IPSPs were recorded with 20 mM Cl^- in the pipette solution. ** Paired-pulse ratio measured with 100 ms interpulse interval.

distances > 100 μm, we estimated it in the four volumes shown in different colours in Fig. 2*F*. The *Y*-dimension was 200 μm, which is close to the width of neocortical layer 2/3. The calculated total number of pyramidal cells (N) in each volume is depicted in the upper panel of Fig. 2*F*. In the lower panel, the calculated number of pyramidal cells connected to the central cell in each volume is shown by bars of corresponding colours, while connection probability is indicated by black rectangles. Note that the number of connected pyramidal cells increased with distance although their relative fraction decreased rapidly. Within a cylindrical volume of 400 μm × 200 μm containing 2512 pyramidal cells, the central cell may receive inputs from 58 other pyramidal cells, giving an average connection probability of about 2 %.

Pyramidal–FS cell connectivity

A comparative mapping of pyramidal cell–FS interneuron pairs (n = 243) is shown in Fig. 3*A*. In most cases, pyramidal cells innervated FS interneurons (red triangles). Moreover, the majority of connections were reciprocal (green filled triangles). Blue triangles correspond to unidirectional inhibitory connections. Figure 3*B* shows the central part of the map with dimensions similar to those in Fig. 2*B* for pyramidal cell pairs. The broad distributions of reciprocally connected cells in both the *X*- and *Y*-directions (Fig. 3*C*) indicate that FS interneurons communicate with most neighbouring pyramidal cells. Moreover, the efficacy of both excitatory and inhibitory synaptic connections was relatively high (Fig. 3*D*). Note, however, that the IPSPs in this distribution were measured with 20 mM Cl^- in the pipette solution. A lower Cl^- concentration in intact cells results in a lower conductance of $GABA_A$ receptor channels. The high connectivity between pyramidal cells and interneurons indicates once again that the pyramidal cell axons were mainly intact, at least within the region of the local network examined.

To estimate the number of pyramidal cells synaptically connected with the interneuron, we performed calculations analogous to those made for pyramidal cells above (Fig. 3*E*). The probability of both excitatory and inhibitory connections varied only slightly with distance, being in the range 0.5–0.75, though the probability of reciprocal connections decreased from 0.52 to 0.25. In a cylindrical volume of 200 μm × 200 μm containing 628 pyramidal cells, we calculated that 492 pyramids innervate a given interneuron, 487 pyramids receive inhibitory inputs from the same interneuron, and 432 pyramids are reciprocally connected to this interneuron. Within the same volume, a pyramidal cell may receive synaptic inputs from only 33 other pyramidal cells.

Summation of unitary synaptic signals in pyramidal–FS cell pairs

Excitatory transmission between pyramidal cells and in pyramidal–FS cell pairs displayed considerably faster postsynaptic potentials compared to inhibitory transmission (Table 1). The relatively fast dynamics of EPSPs resulted in a less prominent summation than that of IPSPs. Figure 4 demonstrates profiles of postsynaptic potentials (normalized to the maximum amplitude), induced by the same random pattern of APs (20 ms minimum interpulse interval) in presynaptic cells, in three types of connection. Pyramidal cells show efficiently summating EPSPs in the beginning of the train, although synaptic depression prevailed later on. Paired-pulse depression in pyramidal–pyramidal connections measured with 100 ms interpulse intervals was moderate (Table 1). Additionally, in 37 % of

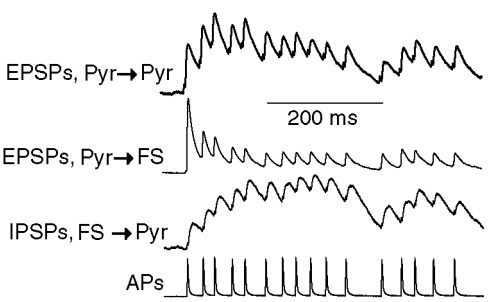

Figure 4. Summation of unitary EPSPs and IPSPs in pyramidal–pyramidal and pyramidal–FS cell pairs

Postsynaptic potential profiles in three types of connection induced by a random pattern of APs in presynaptic cells. Traces represent the average of 50–100 sweeps normalized to the maximum amplitude during the train.

these experiments, paired-pulse facilitation was observed. In the interneuron, EPSPs decreased quickly after the first AP, reaching a virtually steady-state amplitude. In contrast, IPSPs, despite showing synaptic depression (Table 1) summated effectively, increasing the signal amplitude for most of the AP pattern.

Cell responses to afferent stimulation

Single-pulse stimulation of L1 or L6 afferents (below, simultaneous stimulation of L1 and L6 is denoted as 'L1, L6'; separate stimulation of L1 and L6 is denoted as 'L1 or L6') induced EPSPs in pyramidal cells over a large range of amplitudes (> 30 mV), which summated sub-linearly (Fig. 5*A*, left). The degree of non-linearity (Fig. 5*A*, right) did not show a strong dependence on the EPSP amplitude, changing from 85 % to 68 % over the amplitude range 3.5–29 mV. Sub-linear EPSP summation of large (about 10 mV) EPSPs has previously been predicted in modelling experiments (Stuart & Häusser, 2001). Partial overlap of fibres activated by L1 and L6 stimulation could, however, also result in sub-linear EPSP summation. We cannot rule out this possibility, although based on the following results we suggest this effect is minimal. Paired-pulse stimulation (200 ms interpulse interval) of L1 and L6 fibres showed the following results. L1–L1 and L6–L6 stimulation displayed paired-pulse depression of 0.85 ± 0.09 ($P < 0.002$, $n = 11$) and 0.86 ± 0.11 ($P < 0.005$, $n = 11$), respectively. Stimulation of L1 after L6 and L6 after L1 showed that

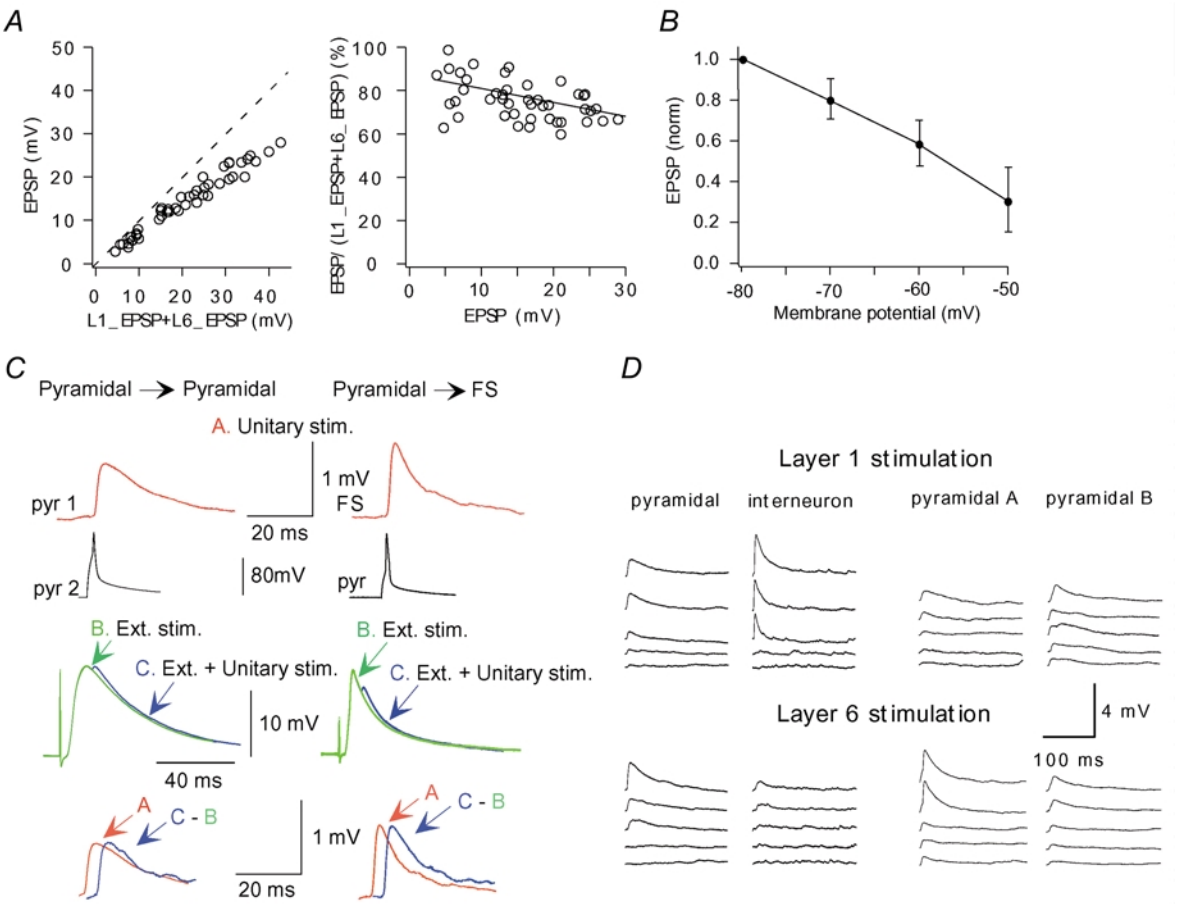

Figure 5. Neuronal responses to afferent stimulation in L1 and L6

A, EPSPs induced in a pyramidal cell by L1 or L6 stimulation summate sub-linearly. Left, EPSPs recorded during simultaneous L1, L6 stimulation are shown *versus* summed EPSPs recorded during separate stimulation of L1 or L6. Right, the degree of non-linearity did not show strong dependence on the EPSP amplitudes, changing from 85 % to 68 % over the amplitude range 3.5–29 mV. *B*, dependence of EPSP amplitudes, evoked by extracellular stimulation (Ext. stim.), on membrane potential. EPSPs were normalized to EPSP amplitude at −80 mV. *C*, transient membrane depolarization initiates mechanisms supporting unitary EPSPs. Unitary EPSPs (A) were recorded in pyramidal–pyramidal and pyramidal–FS cell connections. Large EPSPs (B) were induced by L1, L6 stimulation. Then unitary EPSPs were recorded on the background of large EPSPs induced by L1, L6 stimulation (C). Lower traces compare unitary EPSPs (A) with those extracted from C. *D*, incrementing (30 μA step) stimulation of L1 or L6 afferent fibres induced simultaneous responses in synaptically connected cells in pyramidal–FS and pyramidal–pyramidal pairs. Each trace shows the average of 10–30 sweeps.

EPSP amplitude was not significantly changed by the prior stimulation of the other neocortical layer. L1 stimulation-evoked EPSP amplitudes after L6–L1 stimulation were similar to the first EPSPs in the L1–L1 protocol (ratio 1.01 ± 0.07, $P > 0.5$, $n = 11$); and L6 stimulation-evoked EPSP amplitudes after L1–L6 stimulation were similar to the first EPSPs in the L6–L6 protocol (ratio 1.03 ± 0.08, $P > 0.2$, $n = 11$). Importantly, in all these experiments, a cyclical pattern of stimulation was used (L1–L1 → L6–L6 → L1–L6 → L6–L1) to prevent possible time-dependent changes. These results suggest that synapses activated by L1 and L6 stimulation were largely independent of each other. Sublinear summation could also result from the activation of interneurons innervating pyramidal cells during simultaneous stimulation of L1 and L6.

Note, in many pyramidal cells, single large (up to 30 mV) EPSPs did not initiate an AP, indicating a high activation threshold. Indeed, in 15 cells with RPs of −70.4 ± 4 mV, (layer 2/3 pyramidal cell RPs *in vivo* are more hyperpolarized, RP = −83.8 ± 5.2 mV; Margrie *et al.* 2002), the activation threshold measured was −39.6 ± 5.4 mV. The activation threshold was close to that induced by current injection in the soma (−42.5 ± 2.02 mV, $n = 9$). The large synaptic depolarization required for the initiation of an AP makes it uncertain to what extent unitary synaptic signalling can influence this process.

Extracellularly evoked EPSPs showed a considerable decrease in amplitude with steady-state membrane depolarization (Fig. 5*B*). To determine the extent to which unitary EPSPs are affected by transient synaptic depolarization, unitary connections were excited on a background of large EPSPs induced by L1 or L6 stimulation (Fig. 5*C*). In pyramidal cell pairs, unitary EPSPs did not change significantly ($P > 0.1$, $n = 6$) being 0.81 ± 0.67 mV in control compared with 1.02 ± 0.86 mV when induced close to the peak of single large EPSPs (13.1 ± 3 mV). In pyramidal–FS cell pairs, unitary EPSPs also did not show a significant change ($P > 0.2$, $n = 4$): they were 3.31 ± 2.78 mV in control and 3.19 ± 2.61 mV close to the peak of single large EPSPs (9.8 ± 1.48 mV). These results suggest that a relatively strong (10–15 mV) transient membrane depolarization induced by synaptic activity initiates mechanisms supporting unitary EPSPs. It is uncertain, however, how larger synaptic depolarization, close to the activation threshold, may affect unitary EPSPs.

In most cases, a subtle, minimal-like stimulation of L1 or L6 afferents simultaneously induced postsynaptic potentials in both synaptically connected cells in pyramidal cell pairs, as well as in pyramidal–FS cell pairs (Fig. 5*D*). This suggests that cells in the local network may receive similar information carried by nerve fibres in L1 and L6 (Lampl *et al.* 1999). Increasing stimulation caused a parallel shift of both the pyramidal cells and interneurons towards the activation threshold.

Reproducing dendritic integration during synaptic activity in slices

For mimicking dendritic integration during intensive synaptic activity as in *in vivo* conditions, we simultaneously applied random stimulation patterns independently to afferent fibres in L1 and L6. Figure 6*A* demonstrates the typical location of extracellular electrodes in the slice, and an example of random stimulation patterns applied to the electrodes.

To confirm that afferent stimulation in a slice resulted in an increased dendritic conductance in pyramidal neurons, we used the following procedure (Fig. 6*B*). Postsynaptic currents (PSC, *a*) and postsynaptic potentials (PSP, *c*) induced by subthreshold random stimulation of L1, L6 were measured. Injection of the PSC-shape scaled current (*b*) via the somatic pipette induced a change in the membrane potential (*d*) approximately similar to the PSP in *c*. Injection of a current ramp (0.2 nA s^{-1}) via somatic pipette induced the voltage change shown in *e*. Then, the current ramp was injected simultaneously either with synaptic stimulation (*f*) or with the PSC-shape current injection (*g*) (membrane potentials during only afferent stimulation (*c*) and PSC-shape current injection (*d*) are shown in red). In each of these experiments ($n = 5$), we observed a drastic difference in the responses shown in *f* and *g*, indicating a large decrease in the cell input resistance during subthreshold synaptic activity. The average slope of voltage responses estimated by linear regression in these cells was about eight times smaller in *f* than in *g*.

Increasing the strength of L1, L6 stimulation could readily initiate pyramidal cell firing (see also Cauller & Connors, 1994). Moreover, the interspike intervals (ISIs) during this firing showed a high degree of variability, characteristic of *in vivo* conditions (Holt *et al.* 1996; Stevens & Zador, 1998). The coefficient of variation was 1.22 ± 0.18 ($n = 39$).

Synaptically connected pyramidal cells reveal different firing during afferent stimulation

Would similar synaptic input received by synaptically connected pyramidal cells (see above) induce similar firing patterns? Interestingly, on reaching activation threshold, pyramidal cells did not display alike firing patterns, even with similar RPs and strength of synaptic inputs (see Fig. 7*A*). The neurons revealed significantly different firing patterns during L1, L6 stimulation, as in the example in Fig. 7*A* (left). ISI distributions (Fig. 7*A*, middle) and ISI return maps (Fig. 7*A*, right) verify the robust difference in cell firing. The mean firing rates were 42.3 and 19.7 Hz. Due to similar patterns of extracellular synaptic stimulation, some APs in the cells were synchronous as demonstrated by the firing cross-correlation in Fig. 7*B*. However, the coefficient of correlation of 0.17 indicates that most of the

APs did not fire simultaneously. The coefficients of correlation obtained in five similar experiments were 0.01, 0.26, 0.18, 0.4 and 0.01. The mean firing rates of pyramidal cells in these experiments are shown in Fig. 7*C*.

Modulation of pyramidal cell firing by individual local interneurons

In the local network, the FS interneuron receives strong excitatory inputs from most surrounding pyramidal cells. There is no doubt that this ensemble excitation can change the firing of the interneuron. Can an individual interneuron modify the firing of pyramidal cells? This was tested by dual recordings in pyramidal–FS cell pairs during L1, L6 stimulation (Fig. 8*Aa*; $n = 6$). The amplitude of unitary IPSPs measured in these experiments (low Cl^- concentration in the pipette solution) at RP was relatively small (1.01 ± 0.49 mV). The size of the IPSPs, however, considerably increased with membrane depolarization (Fig. 8*Ae*), and presumably may be larger during supra-threshold synaptic activity.

Supra-threshold stimulation of afferent fibres induced firing of both pyramidal cells and interneurons. The interneuron firing was prevented by hyperpolarization induced by somatic current injection (to −85 mV in Fig. 8*Ab*, right), and ISIs were measured in the pyramidal cell (Fig. 8*Ac*, right). Then, the interneuron hyperpolarization was stopped and ISIs were measured in the pyramidal cell again (Fig. 8*Ac*, left), and demonstrated a decrease in pyramidal cell firing frequency (mean firing rate was 36 Hz without interneuron activity and 27.7 Hz during the interneuron firing). Corresponding ISI return maps are shown in Fig. 8*Ad*. In six cell pairs, the number of pyramidal cell spikes decreased during interneuron activity ($P < 0.02$), though the mean firing rate was not reduced strongly (from 23.5 ± 10.1 to 20.7 ± 9.6 Hz).

Effect of unitary EPSPs on firing in pyramidal–pyramidal cell pairs

Four pyramidal cell pairs, with the mean amplitude of their unitary EPSPs in the range 0.55–1.2 mV, were tested to explore whether APs in the presynaptic pyramidal cell affect firing of the postsynaptic one. In none of these experiments did we observe such an effect. The average firing rate of the postsynaptic neuron was 21.8 ± 3.8 Hz with firing of the presynaptic one, and 21.9 ± 4.8 Hz

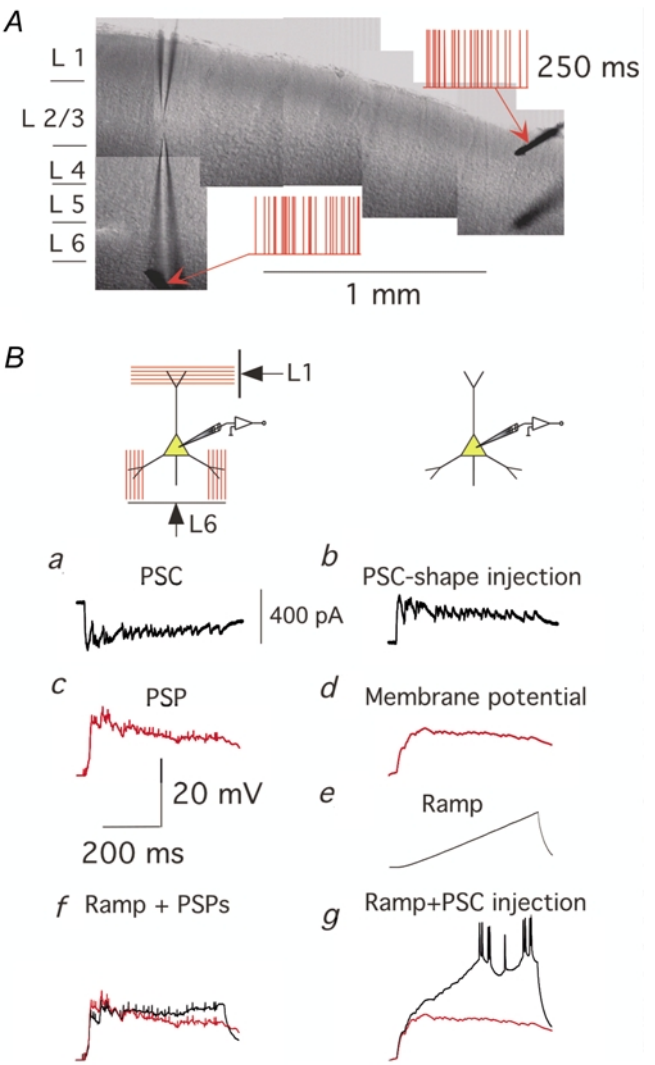

Figure 6. Dendritic integration in slices during intense synaptic activity

A, example of the location of patch pipettes and extracellular electrodes in a slice. Random stimulation patterns applied to the extracellular electrodes are depicted in red. *B*, dendritic conductance is considerably increased during synaptic activity induced by afferent stimulation. *a*, postsynaptic currents recorded in a pyramidal cell during random extracellular stimulation; *b*, corresponding PSC-shape current injected in the same pyramidal cell soma in the absence of afferent stimulation; *c*, postsynaptic potential recorded into a pyramidal cell during random extracellular stimulation; *d*, membrane potential in response to a PSP-shape current injection; *e*, membrane potential in response to a current ramp (0.2 nA s^{-1}) injection; *f*, membrane potential (black) recorded during simultaneous afferent stimulation and current ramp injection (membrane potential during only afferent stimulation is shown in red); *g*, membrane potential (black) recorded during simultaneous injection of PSP-shape current and current ramp (membrane potential during only PSP-shape current injection is shown in red). All traces are the average of 10–20 sweeps.

without it. Figure 8*B* demonstrates one of these experiments when the efficacy of the unitary connection was relatively large (1.2 mV mean EPSP amplitude). The experimental protocol was modified in such a way that either firing of the presynaptic cell was prevented by hyperpolarization or a train of APs (20 Hz) was induced by somatic current injections (Fig. 8*Ba* and *b*). Figure 8*Bc* and *d* shows corresponding ISI distributions and ISI return maps. The mean firing rate was 19.6 Hz with firing of the presynaptic neuron and 19.3 Hz without. Additionally, firing of the postsynaptic cell did not show a correlation with firing of the presynaptic one (Fig. 8*Be*). Here, correlation of the postsynaptic neuron firing with (left) or without (right) presynatic APs was calculated relative to the presynaptic cell firing (see Methods for details).

Effect of unitary EPSPs on interneuron firing in pyramidal–FS cell pairs

Similar experiments in pyramidal–FS cell pairs showed that strong unitary EPSPs are not always effective in modulating interneuron firing. In three experiments (mean amplitude 3.3 ± 1.4 mV), ISIs did not obviously vary during pyramidal cell firing (data not shown). The mean firing rate was 15.7 ± 4.3 Hz during pyramidal cell activity and 15.6 ± 4.3 Hz without it. However, in six other cell pairs (mean EPSP amplitude 4.2 ± 2.1 mV), the interneuron firing was changed significantly by unitary EPSPs: the average firing rate was 28.5 ± 8.8 Hz during firing of pyramidal cells, and 24.4 ± 6.4 Hz without it ($P < 0.01$). Moreover, three pyramidal cells were hyperpolarized to prevent their firing, and triplets of APs (30 Hz) were initiated by somatic current injections (see Fig. 8*Ca* and *b*). Figure 8*C* demonstrates one of these experiments. In addition to the obvious change in the ISI distribution (Fig. 8*Cc*), APs in the pyramidal cell were correlated with the interneuron firing (Fig. 8*Ce*).

DISCUSSION

Local neuronal network in L2/3

We mapped local layer 2/3 pyramidal–pyramidal cell and pyramidal–FS pair connections. In agreement with previous studies of local neuronal connectivity (Mason *et al.*1991; Markram *et al.*1997; Thomson & Deuchars, 1997; Gibson *et al.* 1999; Reyes & Sakmann, 1999; Thomson *et al.* 2002) we found low interpyramidal connectivity, in terms of both the number of unitary connections and the strength of individual connections. In contrast, pyramidal–interneuron connectivity was high, as has been observed previously (Reyes *et al.* 1998; Gibson *et al.* 1999; Thomson *et al.* 2002; Wang *et al.* 2002), with reciprocal connections to the majority of pyramidal cells in the vicinity. A crucial additional parameter obtained in this study was pyramidal cell connection probability as a function of distance. This allowed us to estimate how many other pyramidal cells each network member communicates with, within a particular region. The number of synaptic inputs received by a pyramidal cell from the L2/3 local network neurons is relatively small, about 60 with a distance of ±200 μm.

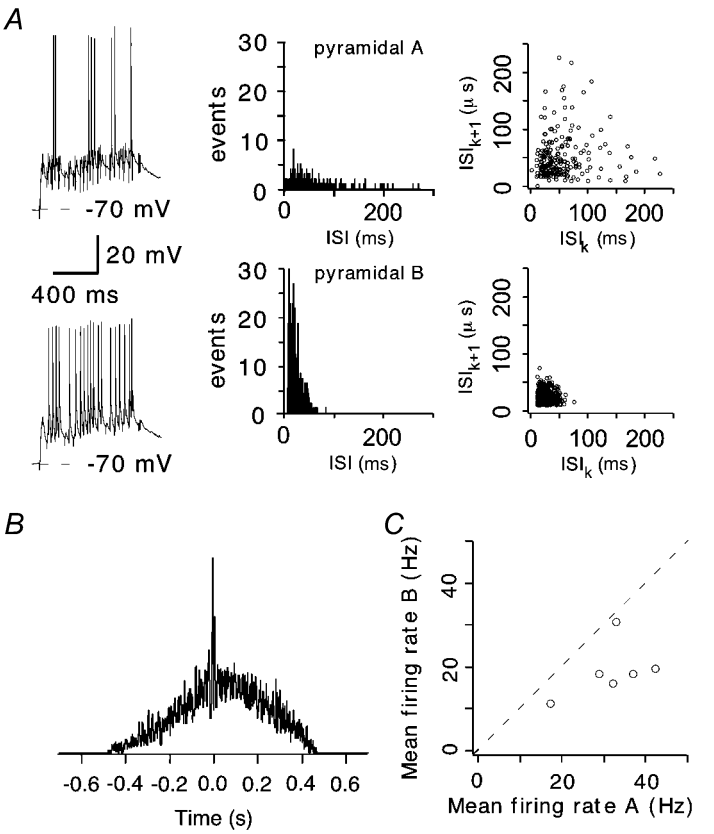

Figure 7. Firing of connected pyramidal cells in response to stimulation of afferent fibres in L1 and L6

A, synaptically connected pyramidal cells reveal distinct firing patterns (left panel) during random L1, L6 stimulation. Note that both the RP and initial strength of postsynaptic responses are similar. Corresponding ISI distributions and ISI return maps are shown in the middle and right panels, respectively. *B*, cross-correlation of AP firing in the pyramidal cells in *A*. *C*, mean firing rates in six pairs of synaptically connected pyramidal cells during L1, L6 stimulation.

These studies were conducted using brain slices from 14- to 16-day-old rats. The question therefore arises; how will development affect neuronal connectivity? The overall pyramidal–pyramidal cell connectivity ratios are difficult to compare with those reported previously in adult animals because of their high variability (Mason *et al.* 1991; Markram *et al.* 1997; Thomson & Deuchars, 1997; Reyes & Sakmann, 1999; Thomson *et al.* 2002) and the lack of connection probability–distance dependence measurements. Other values including cell input resistance, 10–90 % rise time and width at half-amplitude will change with age, as reflected in the faster kinetics of EPSPs and IPSPs measured in older/adult animals (Mason *et al.* 1991; Thomson *et al.* 2002). Additionally, pyramidal–pyramidal cell EPSPs showed paired-pulse depression (with a 100 ms interpulse interval), although 37 % showed slight facilitation. With an increase in age, pyramidal–pyramidal cell EPSP paired-pulse depression changes to paired-pulse facilitation, although EPSP amplitude decreases with age (Reyes & Sakmann, 1999).

Synaptically connected pyramidal cells show different firing patterns

Importantly, in our experiments, communicating pyramidal cells revealed significantly different firing patterns, even

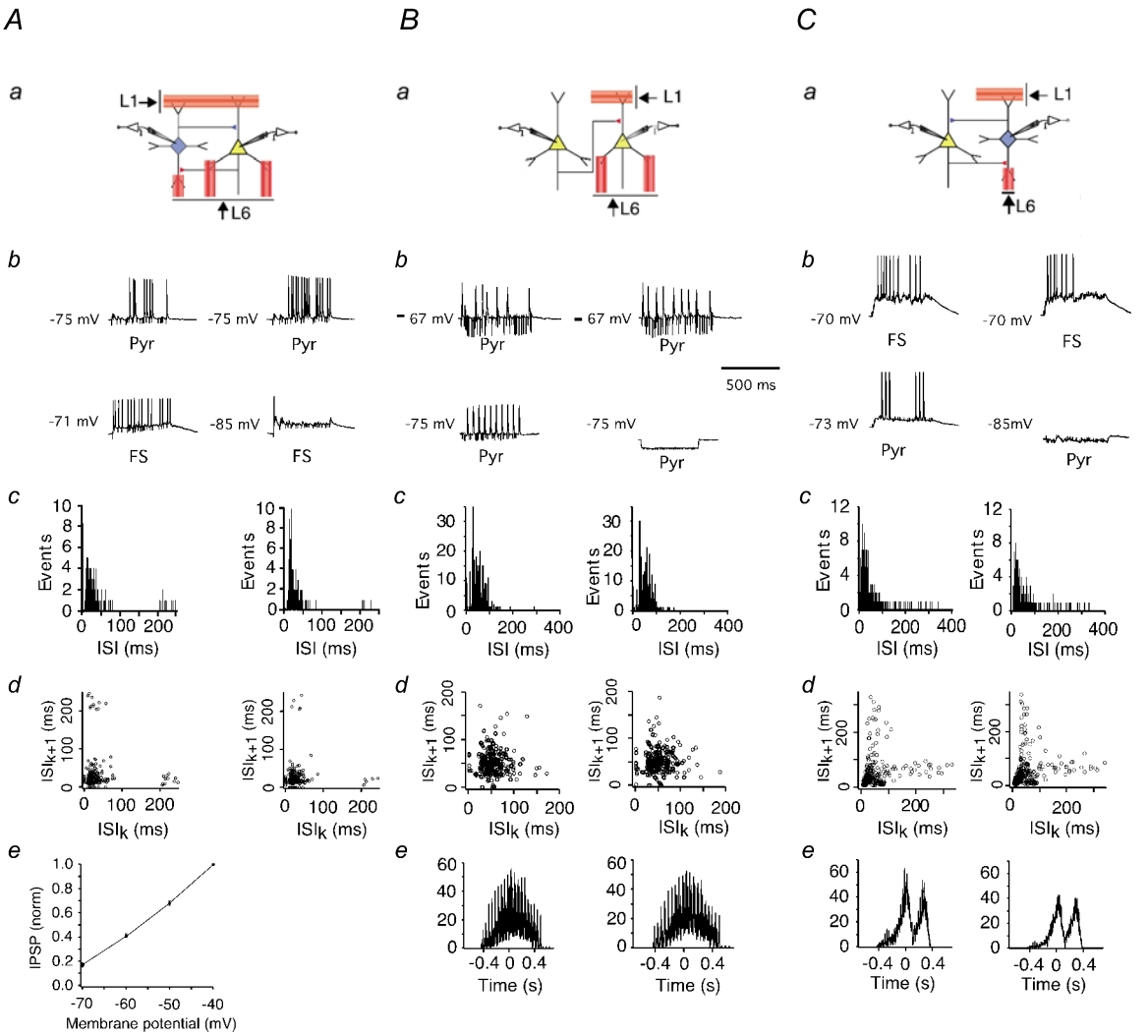

Figure 8. Modulation of cell firing by unitary synaptic signalling

a, schematic diagrams of FS–pyramidal cell (*A*), pyramidal–pyramidal cell (*B*) and pyramidal cell–FS (*C*) microcircuits. *b*, investigation of the effect of unitary PSPs induced by firing of the presynaptic pyramidal cell or interneuron on the firing patterns of the postsynaptic neuron. Firing was initiated either by random L1, L6 stimulation in the postsynaptic neuron (upper panels) and in the presynaptic cell (*Ab*, lower panel) or by somatic current injection (*Bb* and *Cb*, lower panels). Firing of the presynaptic interneurons was prevented by somatic hyperpolarization (lower right panels). ISI distributions (*c*) and ISI return maps (*d*) in the postsynaptic cell were measured with (left) and without (right) firing of the presynaptic neuron. *Ae*, effect of membrane potential on unitary IPSP amplitude. IPSPs were normalized to IPSP amplitude at −40 mV. *Be* and *Ce*, cross-correlograms of neuronal firing with (left panel) or without (right panel) firing of the presynaptic neuron.

with similar RPs and strength of synaptic signalling induced by afferent fibre stimulation (see Fig. 7). This result can be explained by differences in a number of intrinsic cell properties (not studied in the present paper). Moreover, the degree of correlation between cell firing could increase with an increase in the strength of synaptic stimulation (e.g. mean firing rate; Shadlen & Newsome, 1998). *In vivo* recordings show, however, that spontaneous pyramidal cell firing in awake animals is in the range 5–20 Hz (Parnavelas, 1984; Holt *et al.* 1996; Shadlen & Newsome, 1998; Steriade, 2001), or more (> 100 Hz; Softky & Koch, 1993), in response to sensory stimuli. Thus, in our experiments pyramidal cell firing rates were within this physiological range (Fig. 7*C*). A significant difference in firing of adjacent pyramidal cells (not necessarily connected synaptically) obtained in *in vivo* dual recordings was also reported previously (van Kan *et al.* 1985; Gawne & Richmond, 1993; Zohary *et al.* 1994). These results make the possibility that network members may synchronously affect the recipient pyramidal cell questionable.

Effects of unitary connections on cell firing in local microcircuits

The efficiency of unitary synaptic signals in modulating cell firing depends, in particular, on their size and time course. Unitary PSPs are usually measured at RP in quiescent cells. Their properties, however, can vary considerably during transient depolarization and membrane conductance induced by intensive synaptic activity leading to the cell firing. For example, it has been shown recently in modelling studies (Rudolph & Destexhe, 2003) that intensive synaptic activity may cause a strong (up to 80–90 %) attenuation of synaptic signals propagating to the soma. The size of unitary PSPs is generally dependent on the driving force, and thus the electromotive force for currents through AMPA receptor channels decreases with membrane depolarization, negatively affecting the size of EPSPs. Whether this leads to a minimization of the pyramidal cell excitatory effect at the threshold level is as yet unclear (see Fig. 5*C*). It was reported, for example, that the EPSP amplitude might be supported by NMDA receptor channels released from Mg^{2+} block with depolarization (Thomson & Deuchars, 1997) as well as by dendritic Na^{+} channels activated during membrane depolarization (Stuart & Sakmann, 1995; Oviedo & Reyes, 2002). We did not, however, observe modulation of the cell firing by unitary EPSPs in pyramidal–pyramidal cell pairs.

Excitatory connections between pyramidal cells and FS interneurons are much stronger than between pyramidal cells. Nevertheless, pronounced EPSP paired-pulse depression results in weak EPSP summation (see Fig. 4) that decreases the efficiency of unitary EPSPs in modulating interneuron firing. Strong unitary EPSPs did, however, change interneuron firing patterns in most experiments. It was also reported previously that firing of an individual hippocampal pyramidal cell could modulate AP patterns of interneurons *in vivo* (Csicsvari *et al.* 1998; Marshall *et al.* 2002).

Inhibitory connections have an advantage because IPSPs are relatively long lasting (Table 1), facilitating their summation during interneuron firing (see Fig. 4). Besides, the IPSP amplitude increases with membrane depolarization. Presumably, both these properties make a single FS interneuron quite efficient in modulating pyramidal cell firing.

Initiation and modulation of pyramidal cell firing

Within the local network, the limited synaptic signalling received by each pyramidal cell from other network members raises the question of how activity of the network during information processing influences the pattern of firing in the output of a pyramidal neuron. The number of synaptic inputs received by a pyramidal neuron from other network members is relatively small and their efficacy is weak. A significant contribution of pyramidal cells from other neocortical layers is also questionable since the efficacy of these connections has been reported to be very weak (Thomson & Deuchars, 1997; Reyes & Sakman, 1999; Thomson *et al.* 2002). A more likely hypothesis is that pyramidal cell firing is generated on the strong background of synaptic signalling from extra-L2/3 sources (Azouz & Gray, 1999; Destexhe & Pare, 1999; Ho & Destexhe, 2000).

We tested the effects of strong synaptic signalling from extra-L2/3 sources on pyramidal cell and FS interneuron firing properties by stimulating L1 and L6 afferent inputs. Synaptic signalling provided by afferent fibres in L1 and L6 may, however, contain a fraction induced by recurrent axon collaterals of neocortical pyramidal neurons (Vogt, 1984).

If we suggest that computation in the local network is produced by pyramidal cells, their interaction should lead to the modulation of output firing rates. During suprathreshold activity, local pyramidal cells can fire within a similar timeframe. EPSPs evoked in the postsynaptic pyramidal cell by the individual presynaptic pyramidal cell can summate effectively (see Fig. 4). If several presynaptic pyramidal cells fire within the EPSP time window, their activity may be sufficient to modulate the interspike distribution in a target pyramidal cell in spite of the weak efficacy of their connections. On the other hand, modulation of the firing rate can be achieved by pyramidal–interneuron–pyramidal communication. In this context, communication implies a modulation of ISIs, which can be achieved via either excitatory or inhibitory inputs. Thus, the number of interacting pyramidal cells may be considerably increased if we suggest that pyramidal cells communicate not only directly but also via the local

interneurons. Indeed, in this case the number of communicating pyramidal cells is at least 10-fold higher.

Possible functional role of local interneurons

In layer 2/3, at least four different types of interneuron have been found to form reciprocal connectivity with pyramidal cells (Buhl *et al.* 1997; Markram *et al.* 1998; Reyes *et al.* 1998; Zilberter, 2000; Rozov *et al.* 2001; Wang *et al.* 2002). It was also shown that a pyramidal cell might be simultaneously connected with more than one type of interneuron (Markram *et al.* 1998; Reyes *et al.* 1998). Importantly, the properties of pyramidal–interneuron synaptic transmission differ considerably depending on the interneuron type (Markram *et al.* 1998; Reyes *et al.* 1998). For example, bitufted interneurons (Reyes *et al.* 1998) receive strongly facilitating excitatory input from pyramidal cells. Because of this, a train of APs in a single pyramidal cell can initiate an AP in the interneuron (Kaiser *et al.* 1999). In contrast, multipolar interneurons (Reyes *et al.* 1998) receive strongly depressing, although highly efficacious, excitatory input from pyramidal cells. Similarly to FS interneurons, both bitufted and multipolar interneurons form reciprocal connections with the majority of neighbouring pyramidal cells (Y. Zilberter, unpublished observation). Thus, pyramidal cells in the local network may form functionally distinct microcircuits with various types of local interneuron, differentially affecting the firing patterns of each other. Besides, local interneurons of different types are frequently connected to each other (Reyes *et al.* 1998; Gupta *et al.* 2000).

A local interneuron incorporated into the pyramidal cell network receives strong excitatory background from extra-L2/3 sources concurrently with pyramids, and interneuron firing is determined to a considerable extent by the mutual activity of a large fraction of these pyramidal cells. Thus, the interneuron output carries information on the common activity of the network and this information is delivered back to a number of network members, affecting their firing patterns and thereby coordinating the network activity.

REFERENCES

Azouz R & Gray CM (1999). Cellular mechanisms contributing to response variability of cortical neurons *in vivo*. *J Neurosci* **19**, 2209–2223.

Bernander Ö, Duglas RJ, Martin KAC & Koch C (1991). Synaptic background activity influences spatiotemporal integration in single pyramidal cells. *Proc Natl Acad Sci U S A* **88**, 11569–11573.

Borg-Graham LJ, Monier C & Fregnac Y (1998). Visual input evokes transient and strong shunting inhibition in visual cortical neurons. *Nature* **393**, 369–373.

Buhl EH, Tamas G, Szilagyi T, Stricker C, Paulsen O & Somogyi P (1997). Effect, number and location of synapses made by single pyramidal cells onto aspiny interneurons of cat visual cortex. *J Physiol* **500**, 689–713.

Cauli B, Audinat E, Lambolez B, Angulo M, Ropert N, Tsuzuki K, Hestrin S & Rossier J (1997). Molecular and physiological diversity of cortical nonpyramidal cells. *J Neurosci* **17**, 3894–3906.

Cauller LJ & Connors BW (1994). Synaptic physiology of horizontal afferents to layer I in slices of rat SI neocortex. *J Neurosci* **14**, 751–762.

Connors B & Gutnik MJ (1990). Intrinsic firing patterns of diverse neocortical neurons. *Trends Neurosci* **13**, 99–104.

Csicsvari J, Hirase H, Czurko A & Buzsaki G (1998). Reliability and state dependence of pyramidal cell-interneuron synapses in the hippocampus: an ensemble approach in the behaving rat. *Neuron* **21**, 179–189.

Destexhe A & Pare D (1999). Impact of network activity on the integrative properties of neocortical pyramidal neurons *in vivo*. *J Neurophysiol* **81**, 1531–1547.

Destexhe A, Rudolph M, Fellous J-M & Sejnowski TJ (2001). Fluctuating synaptic conductances recreate *in vivo*-like activity in neocortical neurons. *Neuroscience* **107**, 13–24.

Gabbott PLA & Stewart MG (1987). Distribution of neurons and glia in the visual cortex (area 17) of the adult albino rat: a quantitative description. *Neuroscience* **21**, 833–845.

Gibson J, Beierlein M & Connors B (1999). Two networks of electrically coupled inhibitory neurons in neocortex. *Nature* **402**, 75–79.

Gupta A, Wang Y & Markram H (2000). Organizing principles for a diversity of GABAergic interneurons and synapses in the neocortex. *Science* **287**, 273–278.

Hellwig B (2000). A quantitative analysis of the local connectivity between pyramidal neurons in layers 2/3 of the rat visual cortex. *Biol Cybern* **82**, 111–121.

Ho N & Destexhe A (2000). Synaptic background activity enhances the responsiveness of neocortical pyramidal neurons. *J Neurophysiol* **84**, 1488–1496.

Holt GR, Softky WR, Koch C & Douglas RJ (1996). Comparison of discharge variability *in vitro* and *in vivo* in cat visual cortex neurons. *J Neurophysiol* **75**, 1806–1814.

Kaiser KMM, Zilberter Y & Sakmann B (1999). Dendritic Ca^{2+} influx at single synaptic contacts in bitufted interneurons of rat neocortex. *J Physiol* **518.P**, 144*P*.

Kawaguchi Y (1995). Physiological subgroups of nonpyramidal cells with specific morphological characteristics in layer II/III of rat frontal cortex. *J Neurosci* **15**, 2638–2655.

Lampl I, Reichova I & Ferster D (1999). Synchronous membrane potential fluctuations in neurons of the cat visual cortex. *Neuron* **22**, 361–374.

London M & Segev I (2001). Synaptic scaling *in vitro* and *in vivo*. *Nat Neurosci* **4**, 853–854.

Margrie TW, Brecht M & Sakmann B (2002). *In vivo*, low-resistance, whole-cell recordings fron neurons in the anaesthetized and awake mammalian brain. *Pflugers Arch* **444**, 491–498.

Markram H, Lübke J, Frotscher M, Roth A & Sakmann B (1997). Physiology and anatomy of synaptic connections between thick tufted pyramidal neurones in the developing rat neocortex. *J Physiol* **500**, 409–440.

Markram H, Wang Y & Tsodyks M (1998). Differential signalling via the same axon of neocortical pyramidal neurons. *Proc Natl Acad Sci U S A* **95**, 5323–5328.

Marshall L, Henze DA, Hirase H, Leinekugel X, Dragoi G & Buzsaki G (2002). Hippocampal pyramidal cell-interneuron spike transmission is frequency dependent and responsible for place modulation of interneuron discharge. *J Neurosci* **22**, RC197.

Mason A, Nicoll A & Stratford K (1991). Synaptic transmission between individual pyramidal neurons of the rat visual cortex *in vitro*. *J Neurosci* **11**, 72–84.

Miki T, Fukui Y, Masahiro I, Hisano S & Xie Q (1997). Estimation of the numerical densities of neurons and synapses in cerebral cortex. *Brain Res Protoc* **2**, 9–16.

Miki T, Fukui Y, Takeuchi Y & Itoh M (1995). A quantitative study of the effects of prenatal X-irradiation on the development of cerebral cortex in rats. *Neurosci Res* **23**, 241–247.

Nunez JL, Lauschke DM & Juraska JM (2001). Cell death in the development of the posterior cortex in male and female rats. *J Comp Neurol* **436**, 32–41.

Oviedo H & Reyes A (2002). Boosting of neuronal firing evoked with asynchronous inputs to the dendrite. *Nat Neurosci* **5**, 261–266.

Pare D, Shink E, Gaudreau H, Destexhe A & Lang EJ (1998). Impact of spontaneous synaptic activity on the resting properties of cat neocortical pyramidal neurons *in vivo*. *J Neurophysiol* **79**, 1450–1460.

Parnavelas JG (1984). Physiological properties of identified cortical neurons. In *Cerebral Cortex*, vol. 2, ed. Peters A & Jones EG, pp. 205–239. Plenum Press, New York.

Peters A & Kara DA (1985). The neuronal composition of area 17 of rat visual cortex. I. The pyramidal cells. *J Comp Neurol* **234**, 218–241.

Peters A, Kara DA & Harriman KM (1985). The neuronal composition of area 17 of rat visual cortex. III. Numerical considerations. *J Comp Neurol* **238**, 263–274.

Reyes A, Lujan R, Rozov A, Burnashev N, Somogyi P & Sakmann B (1998). Target-cell-specific facilitation and depression in neocortical circuits. *Nat Neurosci* **1**, 279–285.

Reyes A & Sakmann B (1999). Developmental switch in the short-term modification of unitary EPSPs evoked in layer 2/3 and layer 5 pyramidal neurons of rat neocortex. *J Neurosci* **19**, 3827–3835.

Rozov A, Jerecic J, Sakmann B & Burnashev N (2001). AMPA receptor channels with long-lasting desensitization in bipolar interneurons contribute to synaptic depression in a novel feedback circuit in layer 2/3 of rat neocortex. *J Neurosci* **21**, 8062–8071.

Rudolph M & Destexhe A (2003). A fast-conducting, stochastic integrative mode for neocortical neurons *in vivo*. *J Neurosci* **23**, 2466–2476.

Shadlen MN & Newsome WT (1998). The variable discharge of cortical neurons: implications for connectivity, computaion, and information coding. *J Neurosci* **18**, 3870–3896.

Sharp AA, O'Neil MB, Abbott LF & Marder E (1993). The dynamic clamp: artificial conductances in biological neurons. *Trends Neurosci* **16**, 389–394.

Softky WR & Koch C (1993). The highly irregular firing of cortical cells is inconsistent with temporal integration of random EPSPs. *J Neurosci* **13**, 334–350.

Steriade M (2001). Impact of network activity on neuronal properties in corticothalamic systems. *J Neurophysiol* **86**, 1–39.

Stevens CF & Zador AM (1998). Input synchrony and the irregular firing of cortical neurons. *Nat Neurosci* **1**, 210–217.

Stuart G & Häusser M (2001). Dendritic coincidence detection of EPSPs and action potentials. *Nat Neurosci* **4**, 63–71.

Stuart G & Sakmann B (1995). Amplification of EPSPs by axosomatic sodium channels in neocortical pyramidal neurons. *Neuron* **15**, 1065–1076.

Thomson AM & Deuchars J (1997). Synaptic interactions in neocortical local circuits: dual intracellular recordings *in vitro*. *Cereb Cortex* **7**, 510–552.

Thomson AM, West DC, Wang Y & Bannister AP (2002). Synaptic connections and small circuits involving excitatory and inhibitory neurons in layers 2–5 of adult rat and cat neocortex: triple intracellular recordings and biocytin labelling *in vitro*. *Cereb Cortex* **12**, 936–953.

Vogt BA (1984). The role of layer I in cortical function. In *Cerebral Cortex*, vol. 9, ed. Peters A & Jones EG, pp. 49–80. Plenum Press, New York.

Wang Y, Gupta A, Toledo-Rodriguez M, Wu CZ & Markram H (2002). Anatomical, physiological, molecular and circuit properties of nest basket cells in the developing somatosensory cortex. *Cereb Cortex* **12**, 395–410.

Zilberter Y (2000). Dendritic release of glutamate suppresses synaptic inhibition of pyramidal neurons in rat neocortex. *J Physiol* **528**, 489–496.

Acknowledgements

We thank Drs N. Burnashev, M. Larkum, P. Roland and G. Innocenti for critically reviewing the manuscript. This study was supported by a grant from the Swedish Research Council (K2003-33X-14652-01A).